The effect of temperature on the structural, electronic and optical properties of sp^3-rich amorphous carbon

2008 J. Phys.: Condens. Matter 20 035216

(http://iopscience.iop.org/0953-8984/20/3/035216)

J. Phys.: Condens. Matter **20** (2008) 035216 (6pp) doi:10.1088/0953-8984/20/03/035216

The effect of temperature on the structural, electronic and optical properties of sp^3-rich amorphous carbon

J T Titantah and D Lamoen

TSM, Departement Fysica, Universiteit Antwerpen, Groenenborgerlaan 171, 2020 Antwerpen, Belgium

Received 21 March 2007, in final form 15 November 2007
Published 19 December 2007
Online at stacks.iop.org/JPhysCM/20/035216

Abstract

The effect of temperature on the structural, electronic and optical properties of dense tetrahedral amorphous carbon made of ∼80% sp^3-bonded atoms is investigated using a combination of the classical Monte Carlo technique and density functional theory. A structural transformation accompanied by a slight decrease of the sp^3 fraction is evidenced above a temperature of about 600 °C. A structural analysis in combination with energy-loss near-edge structure calculations shows that beyond this temperature, the sp^2-bonded C sites arrange themselves so as to enhance the conjugation of the π electrons. The Tauc optical band gap deduced from the calculated dielectric function shows major changes beyond this temperature in accordance with experimental results. Energy-loss near-edge structure and band gap calculations additionally reveal a massive destabilization of the of sp^3 bonding phase in favour of sp^2 bonding at a temperature of about 1300 °C which agrees very well with the reported value of 1100 °C.

1. Introduction

Major transformations in tetrahedral amorphous carbon (ta-C) are known to occur at two temperatures [1–3]. Above the temperature $T_1 \sim 1100$ °C, the sp^3 fraction decreases strongly while at a lower temperature T_2 (∼600–700 °C) $\ll T_1$ more subtle structural transformations occur which are not accompanied by a major change in the bonding structure. The annealing of as-deposited ta-C at T_2 leaves the material stress-free meanwhile enabling it to retain its mechanical, optical and bonding properties. For example, Ferrari *et al* [2] observed stress relief and demonstrated using EELS spectroscopy, Raman spectroscopy and optical gap measurements that minimal structural changes were recorded when ta-C was annealed between 600 and 700 °C. Friedmann *et al* [4] developed a process for making thick stress-free ta-C by using pulsed-laser deposition and performing short thermal anneals at 600 °C. Monteiro *et al* [5] observed that when a ta-C film (80% sp^3) was annealed at 600 °C there was a remarkable decrease in the stress.

A large amount of theoretical work has been devoted to generate and study the structural, mechanical and electronic properties of amorphous carbon [1, 6–15] but little is done to understand the thermal (temperatures lower than T_1) behaviour of these computer generated structures. Using Brenner's bond-order potential [16], Belov [1] recently studied the relaxation processes in ta-C via an ion-beam deposition molecular dynamics simulation approach. He reported a complete stress relief at a temperature of ∼700 °C which was attributed to diffusionless structural transformations. He also found that this potential overestimated the temperature T_1 to 2500 K when a cut-off distance of 2.25 Å was used.

The goal of this work is to investigate the correlation between the electronic and optical properties of ta-C and the subtle changes in the bonding structure as a function of temperature. We make use of the Tersoff potential [17, 18] because of its simplicity and we take a cut-off distance of 2.45 Å. This choice of the cut-off distance does not affect the properties of the crystalline graphite and diamond phases of carbon whose properties have been used to parametrize the potential. However, it leads to a dramatic improvement of the sp^3 versus density relation [19] as compared to that obtained with the shorter cut-off distance of 2.10 Å (see [20]). It also leads to a reduction of the amount of isolated threefold-coordinated carbon atoms in the tetrahedral amorphous carbon matrix (less than 30% compared to that reported in [21], i.e. 50%). A similar cut-off of 2.46 Å has also been used for this potential to study the defect structures which

have been observed on a graphite surface as a result of ion implantation [22]. Using Brenner's potential, an increased cut-off distance has also been used to study amorphous carbon deposition processes [6, 23]. Other researchers have used the Tersoff potential to demonstrate a 'patching–tearing' mechanism for the single-wall-to-multiwall transformation of bundles of carbon nanotubes [24]. We generate via a Monte Carlo (MC) procedure amorphous carbon structures at a density of 3.4 g cm^{-3}. This density is quite close to the highest measured density for tetrahedral amorphous carbon of 3.3 g cm^{-3} [25]. In order to get an sp^3 fraction which is typical of ta-C structures, we intentionally adopt this density because a high sp^3 carbon content (80–85%) can only be generated using the Tersoff potential at such densities. The tetrahedral amorphous carbon structure is obtained by quenching liquid carbon from 5000 to 1040 °C. The sp^3-rich structure is then equilibrated at various temperatures and the changes in the bonding structure are explored. Within the density functional theory (DFT), the effect of temperature on the electronic and optical properties is also investigated. We demonstrate how a well-parametrized interatomic interaction potential can be used to monitor the temperature effect on the electronic properties (electronic density of states, energy-loss near-edge structure and optical absorption coefficient). The calculated optical band gaps closely follow the experimentally reported temperature dependence.

2. Computational details

The amorphous carbon structures were obtained by a liquid quench within a Metropolis Monte Carlo scheme. At each MC step each atom is given a random displacement and the resulting total energy change in the system ΔE is calculated. This new position is accepted with a probability $\min[1, \exp(-\Delta E/k_{\mathrm{B}}T)]$, where k_{B} is the Boltzmann constant and T is the temperature in kelvins. We melted a 64 atoms cubic cell at a density of 3.4 g cm^{-3} and at a temperature of 5000 °C using the Monte Carlo technique by exploiting the Tersoff potential [17, 18] with the cut-off distance set at 2.45 Å to correctly locate the second-neighbour coordination shell of ta-C [26] and to improve the sp^3 versus density relation in amorphous carbon. This increased cut-off distance did not lead to any extra overcoordination (less than 5% of the atoms were 5-coordinated). The amorphous carbon structures were obtained by cooling (exponentially along the MC steps) the hot carbon at 5000 °C down to a temperature of 1040 °C well below T_1. From this point on, the quenched structure is subjected to various temperatures for over 100 000 MC steps. At the density of 3.4 g cm^{-3}, structures were also generated under similar conditions for systems made of 108, 256 and 512 atoms and they all showed structural (radial distribution function) and bonding (sp^3 fraction) properties similar to the 64 atoms system. The temperature effects on these properties were also similar.

The sp^3 bonding fractions of the carbon systems were obtained by the nearest neighbour counting technique (within spheres of radius 1.9 Å) which was corrected for non-planarity of the 3-coordinated atoms via the π orbital axis vector analysis (abbreviated by POAV1) as described recently [27, 28]. The radius of 1.9 Å lies in a well-defined minimum of the pair correlation function $g(r)$ situated just beyond the shell of the first neighbours. Within the framework of the local density approximation (LDA) [29], DFT calculations were performed on the 64 atoms systems to investigate the temperature effects on the electronic and optical properties. The calculations were performed using the WIEN2k *ab initio* code [30] which uses the all-electron full-potential(-linearized)-augmented-plane-wave + local orbital method. This code partitions the unit cell into muffin-tin spheres centred on each atom and an interstitial region. The Kohn–Sham orbitals are expanded as linear combinations of spherical harmonics and radial functions within the muffin-tin spheres and as plane waves in the interstitial region. Muffin-tin radii (R_{MT}) are fixed at 1.1 au and the plane-wave cut-off parameter $R_{\mathrm{MT}} \times K_{\max}$ ($K_{\max}$ being the plane-wave cut-off) value of 5.5 is used. 100 k-points are used to sample the full Brillouin zone (i.e. 32 in the irreducible Brillouin zone). The effect of temperature on the electronic structure is investigated through the electronic density of states (DOS) and the energy-loss near-edge structure (ELNES) calculation. Dielectric function calculations are also performed and the effect of temperature on the Tauc optical band gap is explored.

3. Results

3.1. sp^2 bond clustering analysis

The clustering of sp^2 C atoms has been suggested as a possible mechanism for stress reduction during the annealing of non-equilibrium as-deposited ta-C at T_2 [31]. In an attempt to probe the ability of Brenner's empirical potential to predict sp^2 bond clustering in amorphous carbon a recent theoretical study [32] showed that at a temperature of about 700 °C the fraction of sp^2 C atoms bonded to at least two other sp^2 atoms increased considerably. In this work, we investigate the effect of heating on this clustering using the Tersoff potential. We examined the temperature dependence of the number of sp^2 C atoms bonded to at least two other sp^2 atoms for the 64, 108, 256 and 512 atoms systems. Our results clearly show enhanced clustering of sp^2-bonded atoms when ta-C is subjected to a temperature $T_2 \sim 700$ °C for the 64 atoms system. This temperature shifted to 600 °C for the 512 atoms system. The difference is a system size effect. Above T_2 the percentage of such C atoms was always greater than that expected for random systems with similar sp^2 fraction [33].

Another quantity that can give further insight into the nature of the sp^2 bond clustering is the distribution $P_N(R)$ of the end-to-end distance R of all-N-sp^2-atom chains in the ta-C. These are chains of N carbon atoms all of which are 3-coordinated. In the left panel of figure 1 we show how $P_4(R)$ changes with temperature for the 512 atoms system. At 600 °C a large peak at 2.84 Å (corresponding to the third coordination shell in flat graphene sheets) emerges. A similar distribution $P_5(R)$ (of chains of 5 sp^2 atoms) also revealed a peak at about 2.45 Å (corresponding to the second coordination

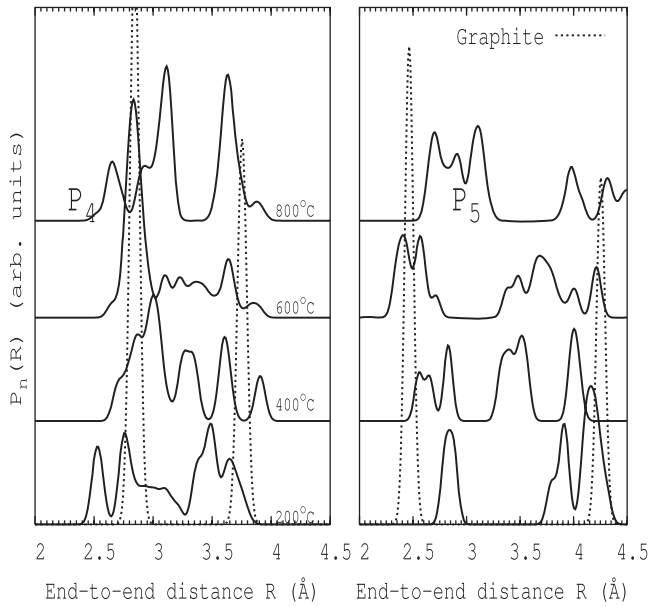

Figure 1. Distribution of the end-to-end distance of chains of 4 sp^2 C atoms (left) and of 5 sp^2 C atoms (right). These are results for the 512 atoms systems which are equilibrated at the indicated temperatures. That of graphite is given for comparison. The area under each curve is normalized to unity. At 600 °C note the huge feature at an end-to-end distance of ∼2.84 Å which corresponds exactly to the third-neighbour coordination shell radius of graphite.

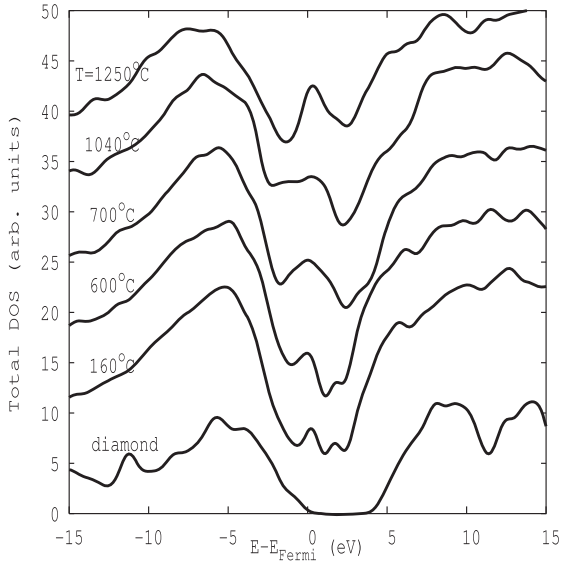

Figure 2. The effect of temperature on the density of states of ta-C. The spectra have been smeared out using Gaussian functions with full width at half maximum of 1.0 eV. The DOS of diamond is given for comparison.

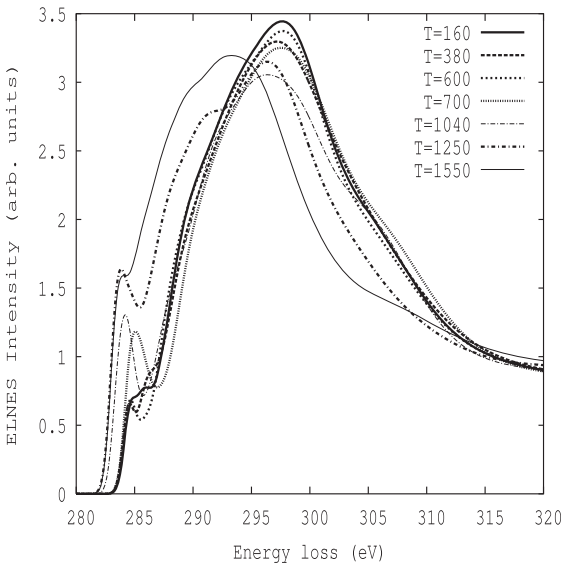

Figure 3. The effect of temperature on the ELNES of ta-C. For temperatures higher than or equal to 700 °C a well-defined π^* peak can be seen which exists only as a shoulder at lower energy loss for lower temperatures. A major increase in the π^* peak intensity is also observed for temperatures greater than T_1.

shell in flat graphene sheets) at this temperature (see right panel of figure 1). The presence of the 2.84 Å feature in P_4 and 2.45 Å feature in P_5 indicate the tendency to form sixfold rings of sp^2 carbon atoms in the ta-C matrix. Thus at 600 °C sp^2 atoms tend to cluster together to form small trigonal, planar graphitic domains. The lack of a prominent feature at 3.75 Å in $P_4(R)$ shows that graphitic domains with a size larger than 3 Å are not present, which is a result of the strong disorder potential characteristic of amorphous carbon systems [34].

3.2. Electronic properties: density of states and energy-loss near-edge structure changes

After equilibrating the system at a given temperature, the final structure was used as input for the DFT calculations. We remark here that the bonding structure of each of the systems remained fairly constant over the equilibration period. The DOS as a function of the equilibration temperature is shown in figure 2. We note the presence of states in the band gap region of diamond (DOS of diamond is also shown). These states are a fingerprint of defective sp^2 carbon atoms. Our local density of states analysis shows that these states correspond to both isolated 3-coordinated atoms and/or neighbouring 3-coordinated carbon atoms of which the p_π orbitals are not parallel.

The local electronic structure is experimentally accessible through ELNES measurements. Therefore we calculated the temperature dependence of these spectra within the sudden approximation (i.e. core–hole effects were not included). It is well known that the effect of core–hole on the C 1s ELNES of carbon systems is the redistribution of the σ^* intensity (where σ^* corresponds to the excitation from the 1s level to the localized σ hybrids). Given the fact that the π^* peak, resulting from the excitation from the 1s level to the delocalized out-of-plane π (p_z) orbital of a trigonally bonded atom, is less sensitive to the core–hole effect [28], the use of the ELNES spectra calculated within the sudden approximation to investigate the changes in the π bonding is adequate. The ELNES spectra shown in figure 3 reveal the following: (i) a π^* peak at about 284 eV and a broad σ^* feature beyond 286 eV, (ii) for temperatures below 700 °C the π^* feature is

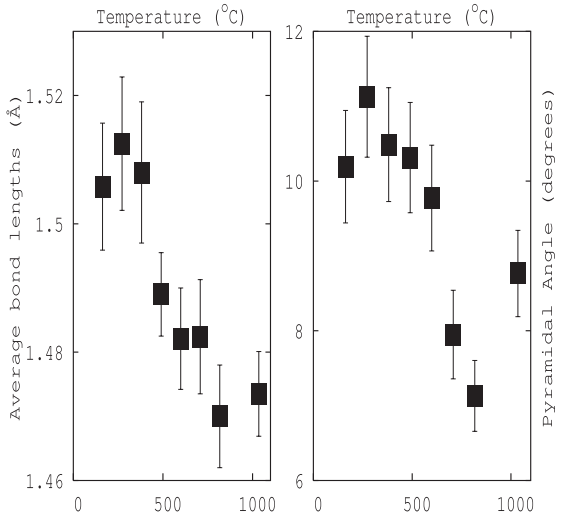

Figure 4. The effect of temperature on the average bond lengths and pyramidalization angle around the 3-coordinated atoms of ta-C. Note the larger bond lengths and pyramidal angles for lower temperatures.

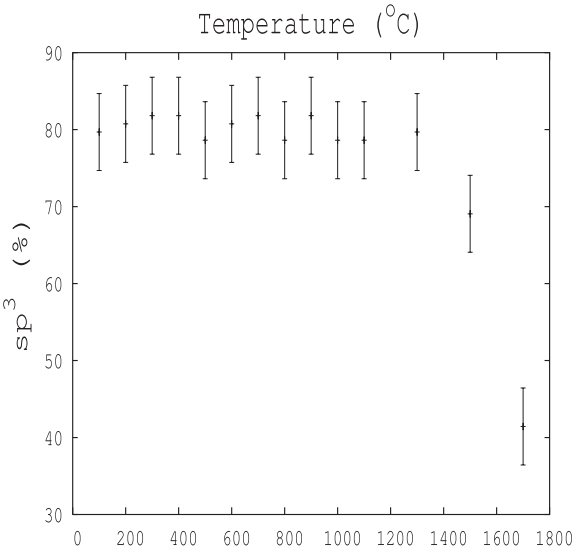

Figure 5. Temperature dependence of the sp^3 fraction of ta-C.

just barely seen, (iii) between 700 and 1200 °C the π^* peak is well defined and a slight increase in its intensity, corresponding to a small decrease in the sp^3 fraction, is recorded above 600 °C, (iv) around $T_1 \sim 1300$ °C there is a drastic increase in the π^* intensity confirming a massive conversion of sp^3- to sp^2-bonded atoms. Characteristic (iii) can be correlated to the ordering of the sp^2-bonded atoms in the ta-C. Within this temperature range the population of delocalized π electrons increases and well-structured π^* features in the ELNES spectra show up. Below T_2 the π^* peak is almost fused together with the σ^* peak. Recently we showed that the σ^* edge onset of sp^2 carbon atoms will shift towards lower energies while the π^* onset remains unaffected when the bond length stretches to longer values [35]. The overlap of the π^* and the σ^* peaks seen below T_2 may thus indicate the presence of stretched sp^2 bonds. In fact the bond length analysis of our computer generated structures reveals that for temperatures below T_2, sp^2 atoms have on the average longer bond lengths (see left panel of figure 4). The overlap may also be indicative of a lack of coplanarity of neighbouring sp^2 orbitals [14, 15, 21, 28]. This lack of coplanarity is analogous to the effect of curvature on the local bonding of 3-coordinated curved carbon systems like the carbon nanotubes and fullerenes. It has been demonstrated that for small diameter carbon nanotubes a curvature-induced hybridization causes the σ^* feature to shift to lower energies thereby overlapping with the π^* feature [28]. For the computer generated amorphous carbon structures the local curvature around a 3-coordinated atom can be defined by the pyramidalization angle of that atom, which is the average angle between the bond vectors of this atom and the plane formed by its three nearest neighbours. This angle varies from 0° (for graphene) to 19.47° (for diamond). The right panel of figure 4 shows that this angle is large for temperatures lower than T_2 and minimal around T_2.

In order to quantify the effect of temperature on the sp^3 fraction we used the POAV1 analysis to calculate the sp^3 fraction of the 512 atoms system as elaborated in [27]. For temperatures lower than 1300 °C the sp^3 fraction remained fairly constant at about $80 \pm 5\%$ but above this temperature this fraction dropped abruptly. Figure 5 demonstrates the variation of the sp^3 fraction with temperature. Using ELNES measurements, Ferrari *et al* [2] observed very similar temperature dependence for a ta-C film with an sp^3 fraction of 85%. Our value of $T_1 \sim 1300$ °C compares quite well with the value of 1100 °C found in that work.

3.3. The effect of temperature on the band gap

From the DFT calculations, optical properties were obtained by using the Optic package [36] of WIEN2k. We used 216 k-points in the irreducible Brillouin zone. Using the Kramers–Kronig relation the real and imaginary parts of the dielectric function were calculated and the optical absorption coefficient $\alpha(h\nu)$ (where h is the Planck's constant and ν is the photon frequency) was deduced as a function of the photon energy $h\nu$. In amorphous systems there is no well-defined band gap which defines the onset of the optical absorption as compared to crystalline materials. Therefore, several methods are used to define an optical band gap [37]. A widely used definition is that given by Tauc *et al* [38]. Under the assumption of (i) parabolic valence and conduction band edges and (ii) a constant momentum matrix element, they showed that the optical absorption coefficient $\alpha(h\nu)$ can be written as

$$\sqrt{h\nu\alpha(h\nu)} = A(h\nu - E_g), \tag{1}$$

where A is a constant. The value of the so-called Tauc gap E_g can be obtained from the energy intercept of a linear fit of $(\alpha h\nu)^{1/2}$ versus $h\nu$. We used for the fitting photon energies between 4 and 7 eV. In figure 6 we show the Tauc plots ($[h\nu\alpha(h\nu)]^{1/2}$) of the absorption coefficient as a function of the photon energy for the ta-C at various temperatures. For energies lower than 3 eV the spectra are characterized by up turns in the intensity. This enhanced absorption activity at low photon energies is once more an indication of a large

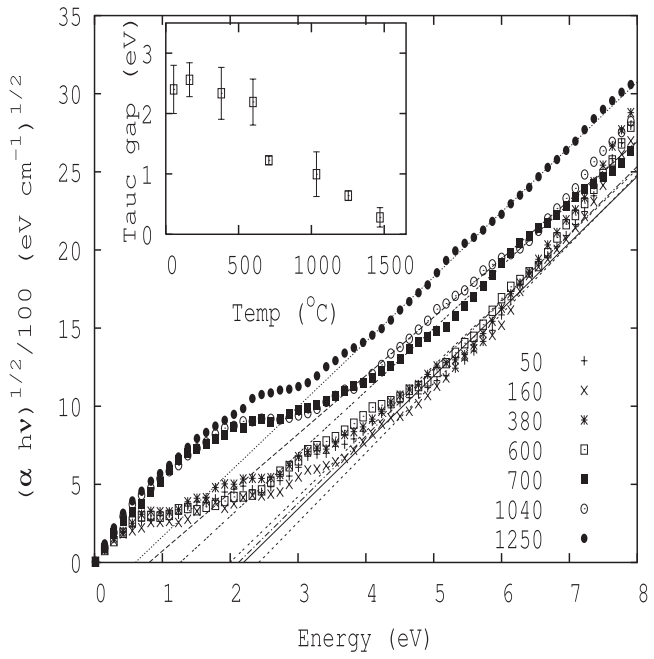

Figure 6. Tauc plot of the optical absorption of ta-C at a density of 3.4 g cm^{-3} at various temperatures in degrees Celsius. In the inset we show the temperature dependence of the Tauc gap. Beyond 700 °C the Tauc gap decreases from about 2.8 eV to less than 2 eV while beyond 1000 °C it is less than 1 eV.

proportion of defect states in the band gap region. For each temperature, it is clearly seen that beyond 4 eV the function $(h\nu\alpha)^{1/2}$ rises linearly with photon energy with a slope which depends on the temperature. The inset in figure 6 shows the variation of the band gap with temperature for the system quenched from 5000 to 1040 °C and allowed to relax at various temperatures. The error bars are obtained by considering fits over two energy windows, 4–6 and 4–8 eV. Below 700 °C E_g is almost constant at 2.5 eV revealing a wide band gap for this temperature range. This is lower than the value of 3.0 eV reported for the Tauc band gap [39] of a ta-C. However, DFT in general, underestimates the true band gaps [40]. The band gap decreases monotonically with increasing temperature and beyond 1000 °C values lower than 1 eV are obtained. The temperature dependence of the Tauc gap obtained in this work is in good agreement with that reported by Ferrari *et al* [2].

4. Conclusion

We have quenched high density liquid carbon from 5000 to 1040 °C and have maintained the resulting structures at various temperatures ranging from room temperature to 1600 °C. We have shown that sp^3-rich amorphous carbon massively converts to sp^2-rich carbon when heated around $T_1 \sim 1300$ °C. Low temperature structural transformations have been shown to be possible for temperatures above $T_2 \sim 600$ °C and lower than T_1. A careful analysis of the local structure shows that this transformation is accompanied by sp^2 bond ordering, whose signature is also clearly seen in the calculated ELNES spectra. For the first time, a systematic theoretical investigation of the temperature effect on tetrahedral amorphous carbon is undertaken via electronic structure and optical absorption calculations. This study demonstrates the strength of using well-parametrized empirical potentials in combination with DFT calculations for the study of the properties of carbon-based materials.

Acknowledgments

This work was supported by the Special Research fund of the University of Antwerp (BOF-NOI) and contract IWT-161 'computational modelling of molecules and materials' of the IWT-Vlaanderen. We also acknowledge financial support from the FWO-Vlaanderen under contract G.0425.05. Calculations were performed on the CalcUA supercomputer of the University of Antwerp.

References

[1] Belov A Y 2003 *Comput. Mater. Sci.* **27** 30
[2] Ferrari A C, Kleinsorge B, Morrison N A, Hart A, Stolojan V and Robertson J 1999 *J. Appl. Phys.* **85** 7191
[3] Krögler H, Ronning C, Hofsäss H, Neumaier P, Bergmaier A, Gorgens L and Dollinger G 2003 *Diamond Relat. Mater.* **12** 2042
[4] Friedmann T A, Sullivan J P, Knapp J A, Tallant D R, Follstaedt D M, Medlin D L and Mirkarimi P B 1997 *Appl. Phys. Lett.* **71** 3820
[5] Monteiro O R, Ager J W, Lee D H, Lo R Y, Walter K C and Nastasi M 2000 *J. Appl. Phys.* **88** 2395
[6] Jäger H U and Belov A Y 2003 *Phys. Rev.* B **68** 024201
[7] McCulloch D G, McKenzie D R and Goringe C M 2000 *Phys. Rev.* B **61** 2349
[8] Kelires P C 1993 *Phys. Rev.* B **47** 1829
[9] Kelires P C 2000 *Phys. Rev.* B **62** 15686
[10] Marks N A, McKenzie D R, Pailthorpe B A, Bernasconi M and Parrinello M 1996 *Phys. Rev.* B **54** 9703
[11] Kaukonen M and Nieminen R M 2000 *Phys. Rev.* B **61** 2806
[12] Smith R and Beardmore K 1996 *Thin Solid Films* **272** 255
[13] Jungnickel G, Köhler T, Frauenheim T, Haase M, Blaudeck P and Stephan U 1996 *Diamond Relat. Mater.* **5** 175
[14] Stephan U and Haase M 1993 *J. Phys: Condens. Matter* **5** 9157
[15] Stephan U, Frauenheim T, Blaudeck P and Jungnickel G 1994 *Phys. Rev.* B **49** 1489
[16] Brenner D W 1990 *Phys. Rev.* B **42** 9458
[17] Tersoff J 1988 *Phys. Rev.* B **38** 9902
[18] Tersoff J 1988 *Phys. Rev. Lett.* **61** 2879
[19] Titantah J T, Lamoen D, Neyts E and Bogaerts A 2006 *J. Phys: Condens. Matter* **18** 10803
[20] Marks N A 2000 *Phys. Rev.* B **63** 035401
[21] Lee C H, Lambrecht W R L, Segall B, Kelires P C, Frauenheim T and Stephan U 1994 *Phys. Rev.* B **49** 11448
[22] Nordlund K, Keinonen J and Mattila T 1996 *Phys. Rev. Lett.* **77** 699
[23] Jäger H U and Albe K 2003 *J. Appl. Phys.* **88** 1129
[24] Lopez M J, Rubio A, Alonso J A, Lefrant S, Méténier K and Bonnamy S 2002 *Phys. Rev. Lett.* **89** 255501
[25] Weissmantel S, Reisse G and Rost D 2004 *Surf. Coat. Technol.* **188/189** 268
[26] Schowalter M, Titantah J T, Lamoen D and Kruse P 2005 *Appl. Phys. Lett.* **86** 112102
[27] Titantah J T and Lamoen D 2004 *Phys. Rev.* B **70** 075115
[28] Titantah J T, Jorissen K and Lamoen D 2004 *Phys. Rev.* B **69** 125406

[29] Perdew J P and Wang Y 1992 *Phys. Rev.* B **45** 13244
[30] Blaha P, Schwarz K, Madsen G K H, Kvasnicka D and Luitz J 2001 *WIEN2k, An Augmented Plane Wave + Local Orbitals Program for Calculating Crystal Properties* (Wien, Austria: Karlheinz Schwarz, Techn. Universität)
[31] Ferrari A C, Rodil S E, Robertson J and Milne W I 2002 *Diamond Relat. Mater.* **11** 994
[32] Belov A Y and Jäger H U 2005 *Diamond Relat. Mater.* **14** 1014
[33] Golzan M M, McKenzie D R, Miller D J, Collocott S J and Amaratunga G A J 1995 *Diamond Relat. Mater.* **4** 912
[34] Robertson J 1995 *Diamond Relat. Mater.* **4** 297
[35] Titantah J T and Lamoen D 2005 *Phys. Rev.* B **72** 193104
[36] Ambrosch-Draxl C, Majewski J A, Vogl P and Leising G 1995 *Phys. Rev.* B **51** 9668
[37] Knief S and von Niessen W 1999 *Phys. Rev.* B **59** 12940
[38] Tauc J, Grigorovici R and Vancu A 1966 *Phys. Status Solidi* **15** 627
[39] Teo K B K, Ferrari A C, Franchini G, Rodil S E, Yuan J, Tsai J T H, Laurenti E, Tagliaferro A, Robertson J and Milne W I 2002 *Diamond Relat. Mater.* **11** 1086
[40] Onida G, Reining L and Rubio A 2002 *Rev. Mod. Phys.* **74** 601